Paper No.
18845

AMPP™
ANNUAL CONFERENCE + EXPO
MARCH 19-23, 2023 | DENVER, COLORADO

Investigations on the Microstructural Stability after Long-term High-temperature Exposure of Alloy 699 XA

Tatiana Hentrich
VDM Metals International GmbH
Plettenberger Straße 2
D 58791 Werdohl
Germany

Heike Hattendorf
VDM Metals International GmbH
Kleffstrasse 23
D 58762 Altena
Germany

Sabine Bellmann
VDM Metals GmbH
Formerstraße 17
D 59425 Unna
Germany

Benedikt Nowak
VDM Metals International GmbH
Kleffstrasse 23
D 58762 Altena
Germany

ABSTRACT

Knowledge of the long-term microstructural stability of a new material is a fundamental requirement for industrial applications operating at temperatures > 500°C. For this reason, microstructural investigations on samples of the newly developed Alloy 699 XA after long-term exposure at temperatures between 500 and 900°C have been performed by scanning electron microscope (SEM). One key application of the new alloy is in the petrochemical industry under metal dusting conditions at high temperatures, underlining the importance of material characterizations presented in this study.

In addition to experimental investigations, thermodynamic calculations have been performed to get an overview of the relevant phases. One focus of the study was on the γ'-precipitation behavior of Alloy 699 XA over durations up to 5000 h. The SEM results showed that the solvus temperature for the γ'-phase is slightly above 800°C, which is in good agreement with the results of mechanical tests on the samples after aging. However, this solvus temperature is higher than the value from thermodynamic calculations (770°C), highlighting the importance of long-term exposure experiments.
Another essential result was that no detrimental, incoherent phases have been found even after 5000 h of exposure at higher temperatures and no continuous occupancy of one of the phases on the grain boundaries, which could have a negative impact on the creep strength of the material.

Key words: Alloy 699 XA, N06699, Corrosion resistant alloys, Nickel alloys, Scanning electron microscopy (SEM), Gamma-prime phase, Phase stability, Metal Dusting, Chemical process industry

INTRODUCTION

VDM[(1)] Alloy 699 XA (UNS N06699, EN Alloy number 2.4842) is a new alloy, which was developed for applications in the petrochemical industry under metal dusting conditions between 400°C and 800°C.[1-3] Important properties of a new material are corrosion resistance, such as to metal dusting, oxidation resistance, and workability versus high temperature strength, which are essential for industrial applications. Currently, there are material solutions which demonstrate good metal dusting resistance, but may have issues with workability. In addition, there are also minimum requirements concerning creep resistance. It is therefore of fundamental interest, in the context of alloy design, to develop materials that has these important properties and satisfies the needs of industrial users.

Another crucial aspect concerning the materials characterization and its application about industrial-relevant operating times is the long-term, high-temperature microstructural stability. It is an important property and has a significant impact on long-term mechanical properties such as creep behavior, corrosion, and oxidation resistance.

Thermodynamic calculations provide a first overview of the relevant phases and phase volumes, but for a detailed analysis of the microstructure, including precipitations morphology, experimental investigations are necessary., For example, the γ'-precipitation behavior over longer periods of time for a 2 % aluminum containing alloy like Alloy 699 XA. In this study, the microstructural investigations on samples after long-term exposure up to 5000 h at different temperatures are performed by Scanning Electron Microscope (SEM). The mechanical properties are evaluated by tensile tests. The precipitation behavior of carbides as well as the γ'-phase were studied and evaluated depending on temperature and exposure time.

EXPERIMENTAL PROCEDURE

Alloy and Production Route

The chemical composition of Alloy 699 XA (heat no. 319144) is shown in Table 1. The heat was melted in an electrical furnace and electro slag remelted (ESR). Then hot rolled and solution annealed plate of 25 mm thickness was produced. From this plate, blanks of, 210 x 40 x 25 mm coupons were cut. Long-term aging exposures in air at 500, 550, 600, 650, 700 and 750°C each for 200, 2000 and 5000 h, at 800 and 900°C each for 200 and 2000 h as well as at 1000°C for 200 h were performed. From these blanks the samples for the examinations were cut.

Table 1
Composition of the heat of Alloy 699 XA used in this investigation.

heat	C	N	Cr	Ni	Mn	Si	Ti	Nb	Fe	Al	Zr	Other
319144	0.02	0.017	29.5	68.0	<0.01	0.1	0.01	0.1	0.15	2.1	0.03	<0.1

Phase calculations

Phase calculations were performed with JMatPro[(2)] V13[4] simulation software on Alloy 699 XA using the composition in Table 1.

[(1)] Trade name
[(2)] Trade name

Tensile test at room temperature

Room temperature tensile tests according to DIN[(3)] EN ISO 6892-1[5] were performed on all long-term aged samples and on samples in the solution annealed condition.

SEM Examinations

SEM examinations were done on solution annealed samples and on the samples aged at 500, 550, 600 and 700°C for 5000 h, and at 800 and 900°C for 2000 h. Since the focus of this study was on metallographic examinations, three different etching mediums were used for the investigations. By using the etching medium Hydrochloric-Nitric-Acid, it is possible to analyze general characteristics of the microstructure, i.e. the grain size distribution and general precipitations sizes as well as their distributions. This medium does not affect precipitations so they are not etched out by Hydrochloric-Nitric-Acid. However, since Alloy 699 XA contains both types of precipitations (carbides and γ′-phase) as grain boundary precipitates, two additional etching mediums (Canada's and Murakami's etchant) were applied.[6] Canada's etchant etches out the γ′-phase without etching the matrix, the grain boundaries or the carbides. By using Murakami's etchant only carbides, nitrides and carbo-nitrides can be analyzed without affecting the matrix, grain boundaries or γ′-phase.

Table 2
Overview table of the different etching methods (RT = room temperature).

Etching medium	Formula and etching parameters	Etching effect
Hydrochloric-Nitric-Acid	60 ml HCl, 10 ml HNO_3, RT, about 30 sec.	Surface etching: grain boundaries, matrix is etched. Precipitations of γ′-phase as well carbides still remain.
Canada's etchant	80 ml H_2O, 20 ml H_2SO_4, 20 ml HF, 10 ml HNO_2, RT, 5 min.	Matrix, grain boundaries are not affected. Carbides remain. Only γ′-phase is etched out.
Murakami's etchant	100 ml H_2O, 10 g NaOH, 10 g $K_2(Fe(CN_6))$, RT, 10 min.	Matrix, grain boundaries are not affected. γ′-phase remain. Only carbides are etched out.

In order to achieve a higher contrast in the SEM figures, InLens and SE detectors were used for the analysis depending on the surface quality of the samples. Both detect the secondary electrons that are used to image the surface of the samples. For the InLens detector the focus of the electron beam is shifted upwards, in comparison to the SE detector. This means that only the uppermost layer of the sample surface is analysed.[7] Because both types of detectors were used in this study, two figures from the same position but with different detectors (InLens and SE) have been taken and can be compared (see Figure 1). The contours of the precipitations are brighter in figures taken by using the InLens mode compared to the SE mode due to the irradiation effect at the edges of the precipitations. This effect is caused by the difference in surface topography, as electrons are emitted not only from the surface of the particles but also from their side edges. Figures taken by the SE detector do not show this effect, since the focus of the electron beam is closer to the sample surface and as a result, more emitted electrons from deeper-lying material regions are detected, since the excitation bulb is deeper as well compared to the InLens mode. Hence, this irradiation effect is not observed for the SE mode. In addition, this effect can be observed on the matrix surface after etching with Hydrochloric-Nitric-Acid (6:1), since the matrix cannot be etched completely homogeneously (see Figure 2). Based on local surface tension states as well as grain orientations, the intensity of the etching process can be quite different and vary for different sample surface positions.

[(3)] DIN EN ISO: DIN Deutsches Institut für Normung e. V., Am DIN-Platz, Burggrafenstraße 6, 10787 Berlin; EN European Standard; ISO International Organization for Standardization

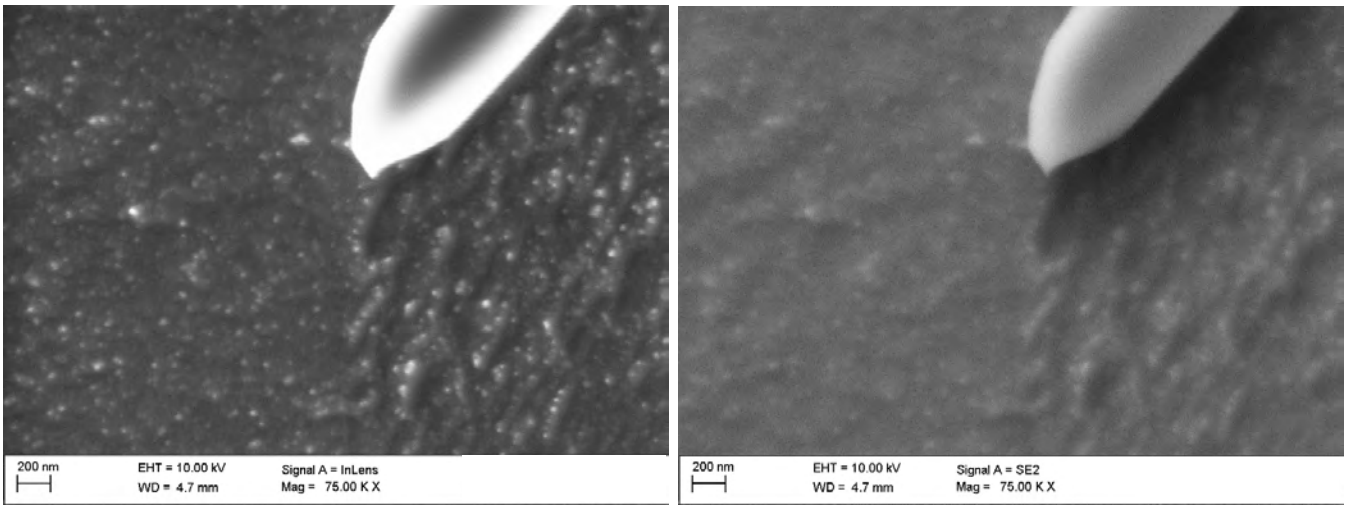

Figure 1: SEM images by using the InLens mode (left) and the SE mode (right) (Hydrochloric-Nitric-Acid (6:1) etching).

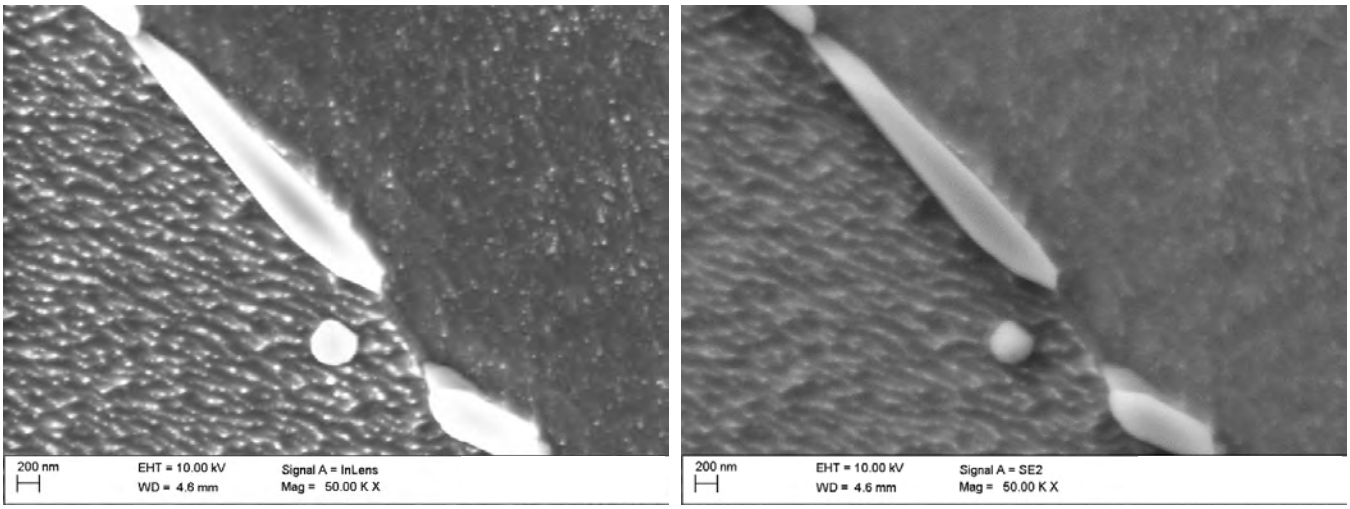

Figure 2: SEM images (left: InLens mode / right: SE mode) to illustrate the different etching intensiyity of Hydrochloric-Nitric-Acid (6:1).

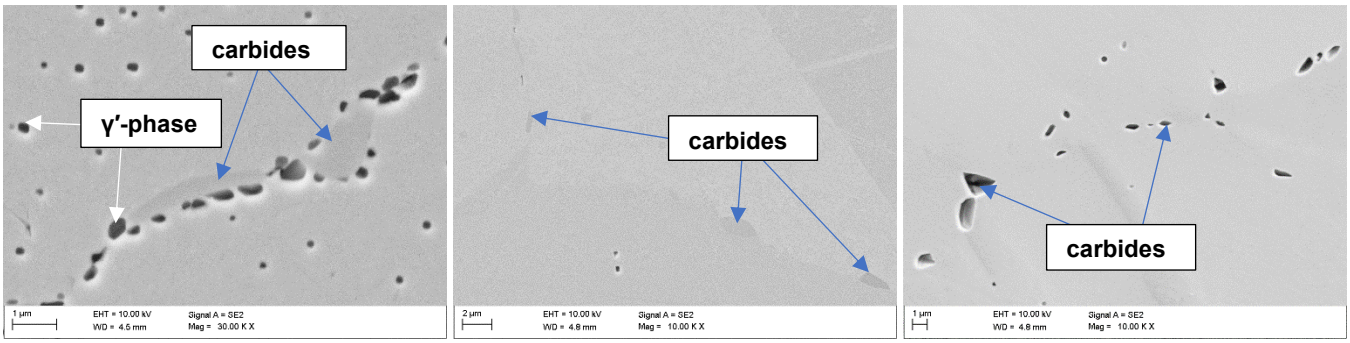

a) b) c)

Figure 3: SEM of the microstructure (SE mode) a) and b) Canada's etching: etched γ′-phase; matrix and carbides still unaffected. c) Murakami's etching: only carbide contours can be seen.

In Figure 3 the different effects of using Canada's and Murakami's etchants can be seen. Figure 3a and b show images with Canada's etching and hence the γ′-phase becomes visible on the grain boundaries and in the grains. The matrix is not affected. It can be seen that two carbide precipitations are present on the grain boundary in Figure 3a. In Figure 3c the carbides contours can be seen due to Murakami's etchant.

Figure 4 illustrates the different appearance of the γ′-phase depending on the etching medium. Since Hydrochloric-Nitric-Acid removes the matrix (left), the γ′-phase still remains in comparison to Canada's etching (right), which removes the γ′-phase.

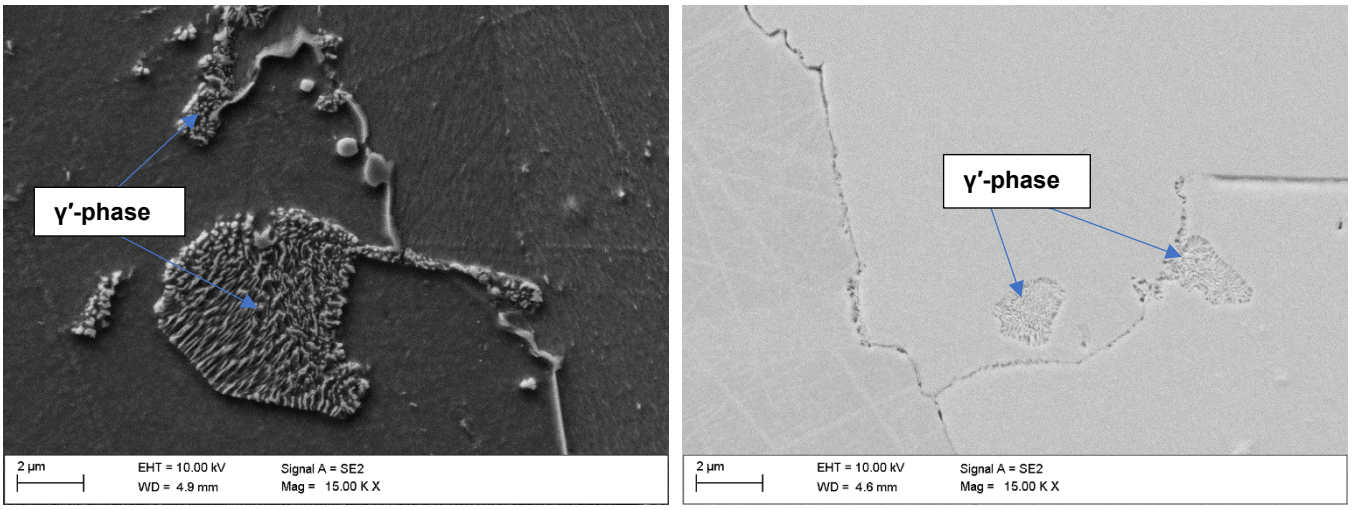

Figure 4: Example of the microstructure of Alloy 699XA using Hydrochloric-Nitric-Acid etching (left) and by using Canada's etching (right). SEM image using the SE mode.

RESULTS

Thermodynamically calculations – TTT diagram

Figure 5 shows the calculated phases, which are thermodynamically stable in Alloy 699 XA. The following phases are predicted: liquid, austenitic gamma γ, gamma prime γ' ($(Ni,Ti)_3Al$) below 770 °C, carbides $M_{23}C_6$ below 1130°C and nitrides (MN). During long-term annealing metastable phases may be precipitated and dissolved again.

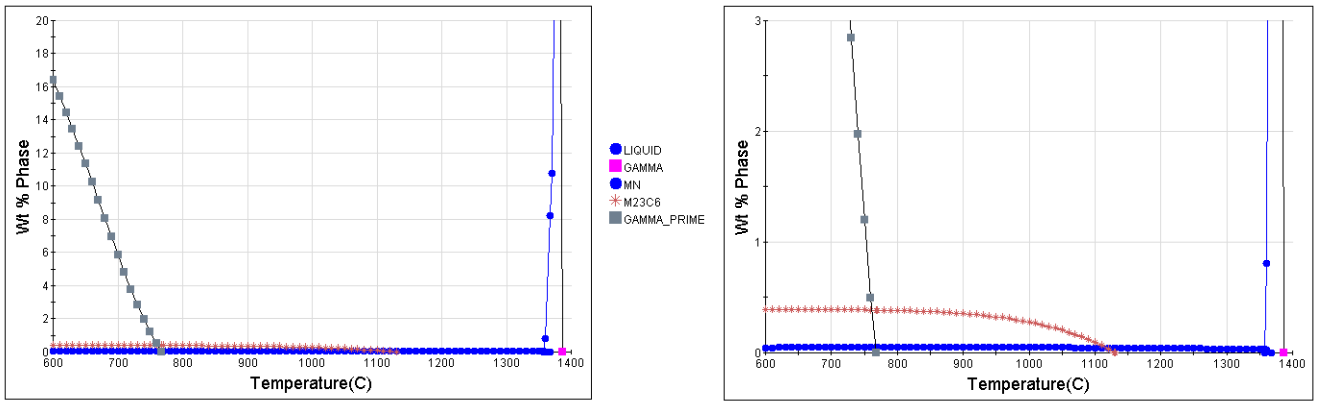

Figure 5: Phase diagrams for Alloy 699 XA calculated with JMatPro.

For this reason the time-temperature-transition (left) and the continuous-cooling-transformation diagram (right) as shown in Figure 6 for Alloy 699 XA, are useful to evaluate the time-dependent precipitation

behavior over time correctly. In contrast to the calculations in Figure 5 these kinds of simulations are not calculated in the thermodynamic equilibrium. In addition to $M_{23}C_6$ carbides, M_7C_3 carbides are also predicted. One important point of interest in real long-term material application is that no detrimental phases appear, but also that the morphology of existing phases does not become detrimental for important properties, i.e. metallurgical creep. Therefore, experimental long-term exposure experiments on materials are crucial and needed in order to prove and verify these calculations, which is also a motivation of this study. The samples annealed between 500 and 700°C are in the region of γ'-phase and additionally carbide precipitations. The samples annealed at 800°C and 900°C are in the region of only carbide precipitations.

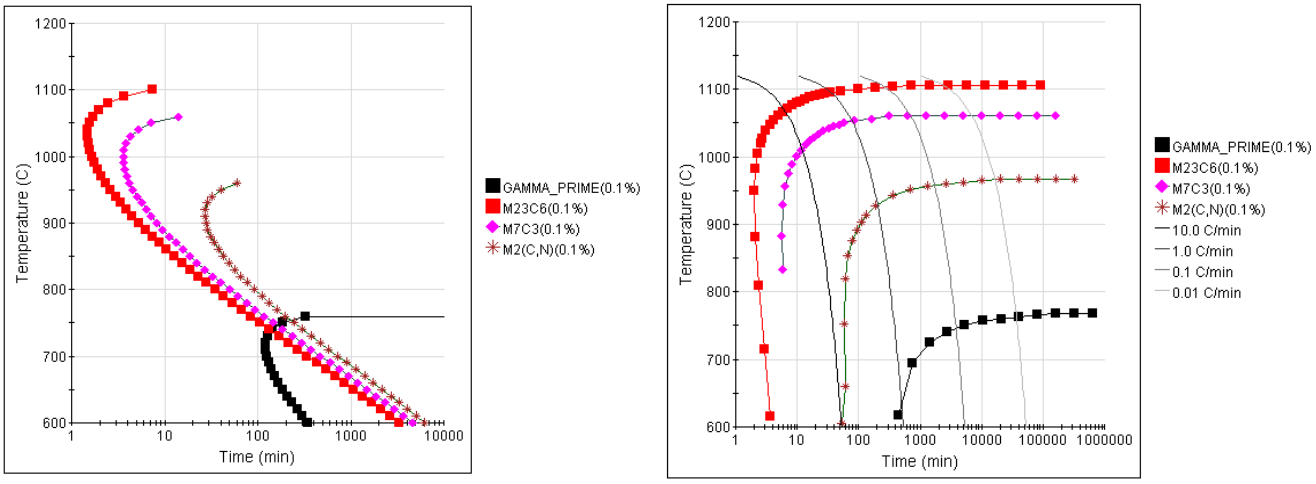

Figure 6: Time-temperature-transition diagram (left) and continuous-cooling-transformation diagram (right) for Alloy 699 XA calculated with JMatPro.

Yield strength at room temperature

Figure 7 shows the results of tentile tests on solution annealed and aged samples.[8]

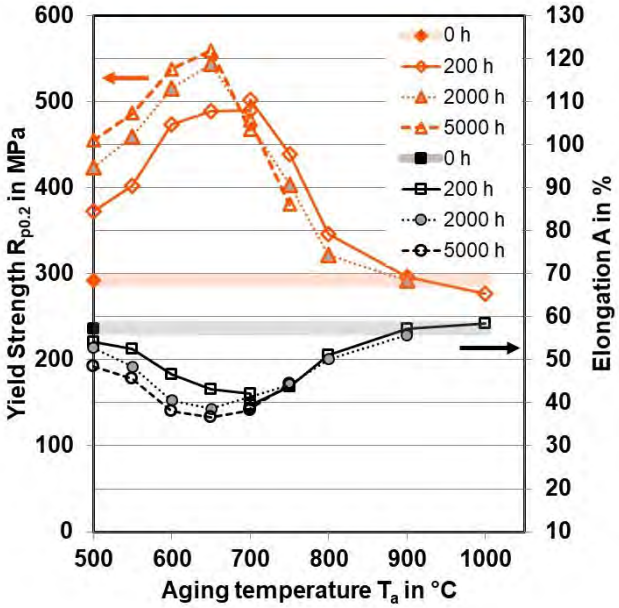

Figure 7: Measured yield strength and elongation at room temperature depending on aging temperature for different aging times of solution annealed samples of Alloy 699 XA.[8]

Up to 650°C the yield strength increases and the elongation decreases with increasing annealing time. Above 700°C until 800°C the yield strength first increases and then decreases with increasing annealing time. Above 700°C the elongation first increases and then shows only minor changes with increasing annealing time. Above 900°C, the influence of aging time on yield strength and elongation is only minor. The maximum for the yield strength and the minimum of the elongation respectively for 200 h is at about 700°C and at about 650°C for 2000 and 5000 h. The phase diagrams in Figure 6 and 7 indicate that γ'-precipitations form below about 770°C, which is the reason for the inrceasing yield strength (decreasing elongation) below 700°C due to an increasing number of small, growing precipitations.[9] Up to 650°C the exposure time was not long enough to cause overaging (decreasing number of coarser precipitations). Above about 700°C overaging of the precipitation started within the examinated aging time and a maximum in yield strength can be identified.

Microstructure investigations

The sample in the solution annealed condition in Figure 8 shows a homogeneous distribution of the carbides on the grain boundaries and in the grains. Some small angle grain boundaries can be observed. A different topography of the sample surface can be seen based on grain orientation and following etching behavior.

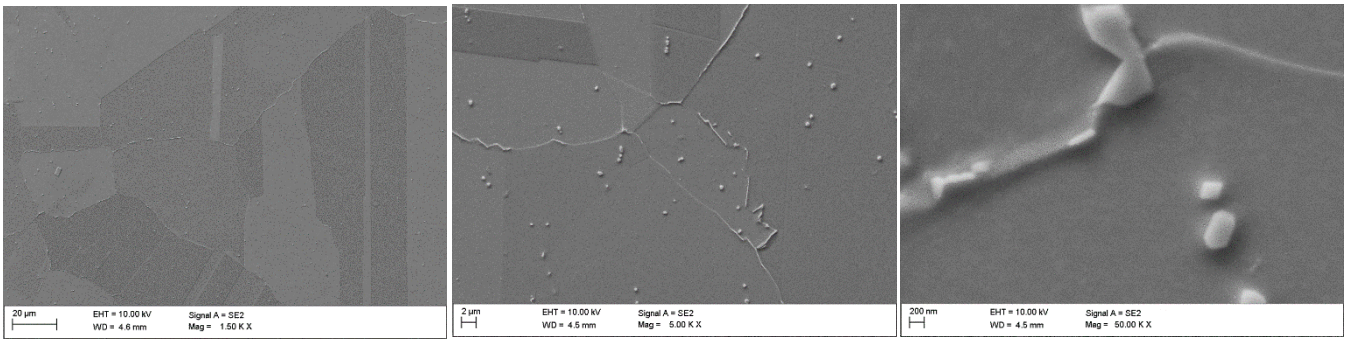

Figure 8: SEM images by using the SE mode and Hydrochloric-Nitric-Acid (6:1) etching of a sample in the solution-annealed condition.

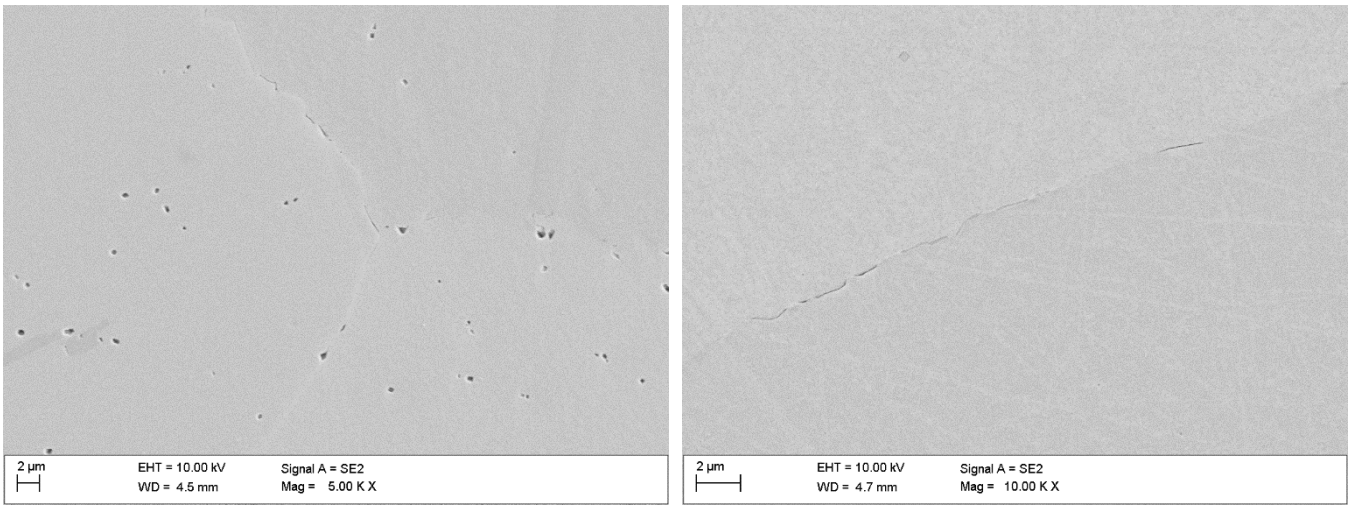

Figure 9: SEM images by using the SE mode and Murakami's (left) and Canada's etching (right) of a sample in the solution-annealed condition.

In Figure 9 (right, Canada's etching) only minor small local precipitations of γ'-phase on the grain boundaries probably based on slight segregations can be seen. In the Murakami's etching (left) some small carbides have been etched out.

Aging at 500°C for 5000 h

After an annealing at 500°C for 5000 h a slight increasing of the grain boundary precipitations can be observed. Due to the relatively low temperature, the diffusion driven processes are slowly. In Figure 11 (left, Murakami's etching) carbides can be identified on the grain boundaries as well as in the grains. Some growing of γ'-precipitations through movement of grain boundaries ("zigzag" γ') can be seen on the grain boundaries (Figure 11, right). However, no visible amount of γ'-precipitations in the grains could be detected by using SEM. The investigations in this study have been performed up to a maximum magnification of 100.000x. In order to detect small sized γ'-precipitations in the range of some nano-meters, which might be present in the grains after an annealing at 500°C for 5000 h, more advanced SEM techniques or even TEM are necessary. However, the increase of the measured yield strength after an annealing at 500°C (Figure 7) supports the statement of fine and small-sized γ'-precipitations in the grain.

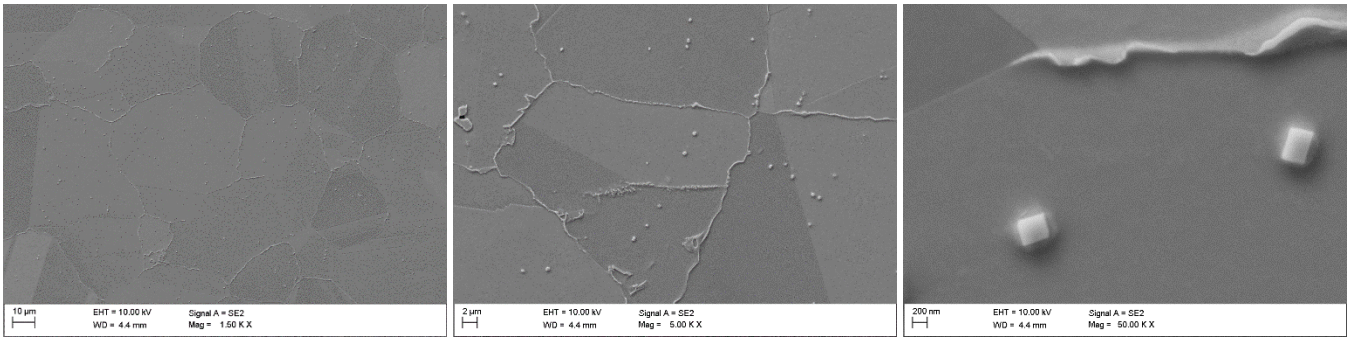

Figure 10: SEM images (SE mode) using Hydrochloric-Nitric-Acid (6:1) etching after an aging of 5000 h at 500°C.

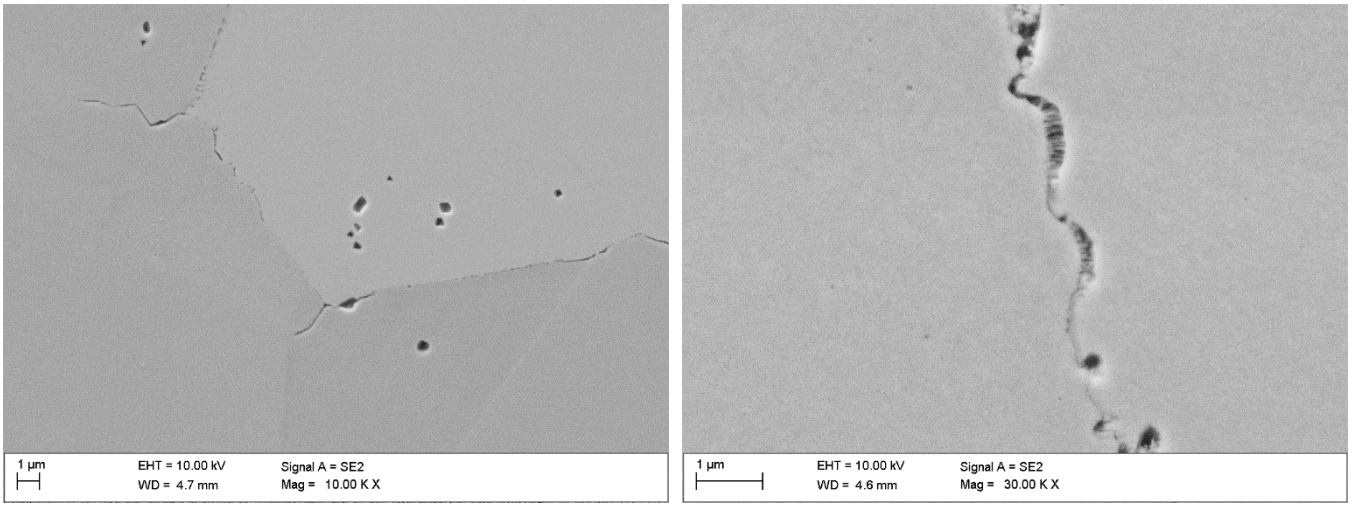

Figure 11: SEM images (SE mode) using Murakami's (left) and Canada's etching (right) after an aging of after 5000 h at 500°C.

Aging at 550°C for 5000 h

The movement of grain boundaries with precipitations of "zigzag" γ' as well as carbides could be observed (Figure 12) very clearly after annealing 5000 h at 550°C. "Zigzag" γ' movement of grain boundaries can

be seen already in images with lower magnifications (see Figure 12, middle and 13). The details can be seen at higher magnifications. Also at 50.00kx magnification no visible γ'-phase in the grains can be detected (Figure 12, right).

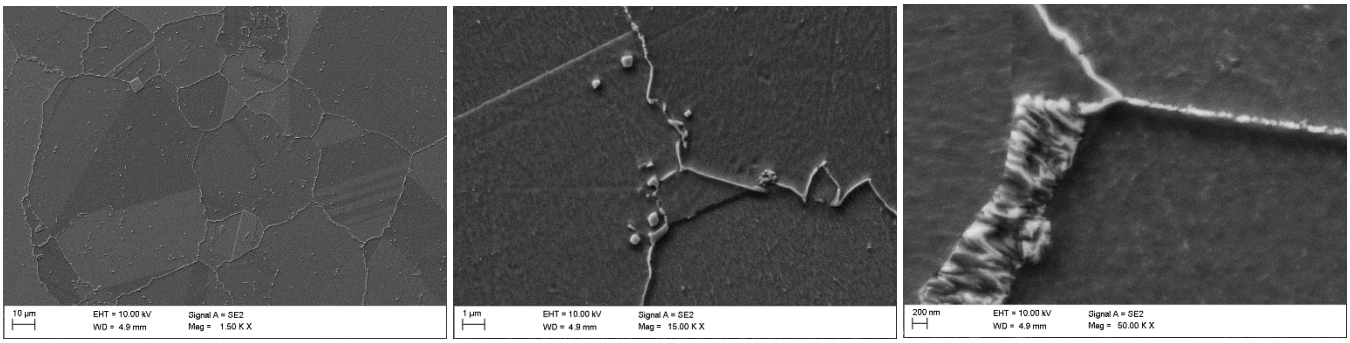

Figure 12: SEM images (SE mode) using Hydrochloric-Nitric-Acid (6:1) etching after an aging of 5000 h at 550°C.

In Figure 13 small y'-precipitations on the grain boundaries can be seen, but no continuous occupancy of one kind of precipitations on the grain boundaries. A continuous precipitation of carbides or γ'-phase could have a negative impact on the creep behavior and reduce the creep strength.[10]

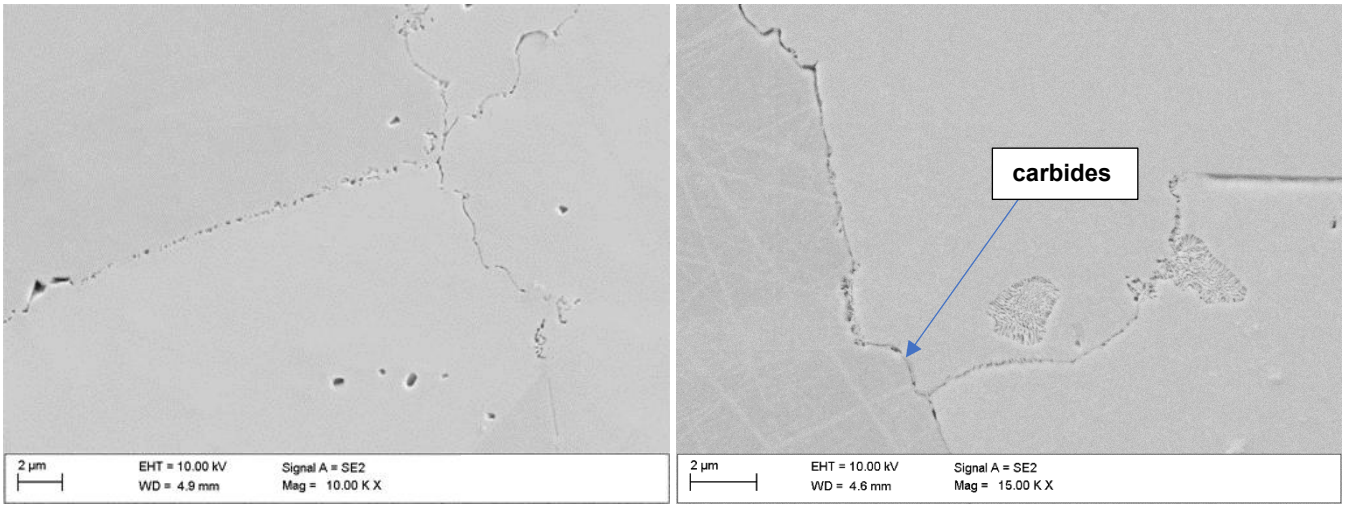

Figure 13: SEM images (SE mode) for Murakami's (left) and Canada's etching (right) after an aging of 5000 h at 550°C.

Aging at 600°C for 5000 h

Grain boundary precipitations and small precipitations of γ'-phase can be observed after an annealing at 600°C for 5000 h (Figure 14-16). A homogeneous distribution of γ'-precipitations in the grains can be seen in the left part of Figure 14. Again the movement of grain boundaries with precipitations of "zigzag" γ' as well as carbides could be observed.

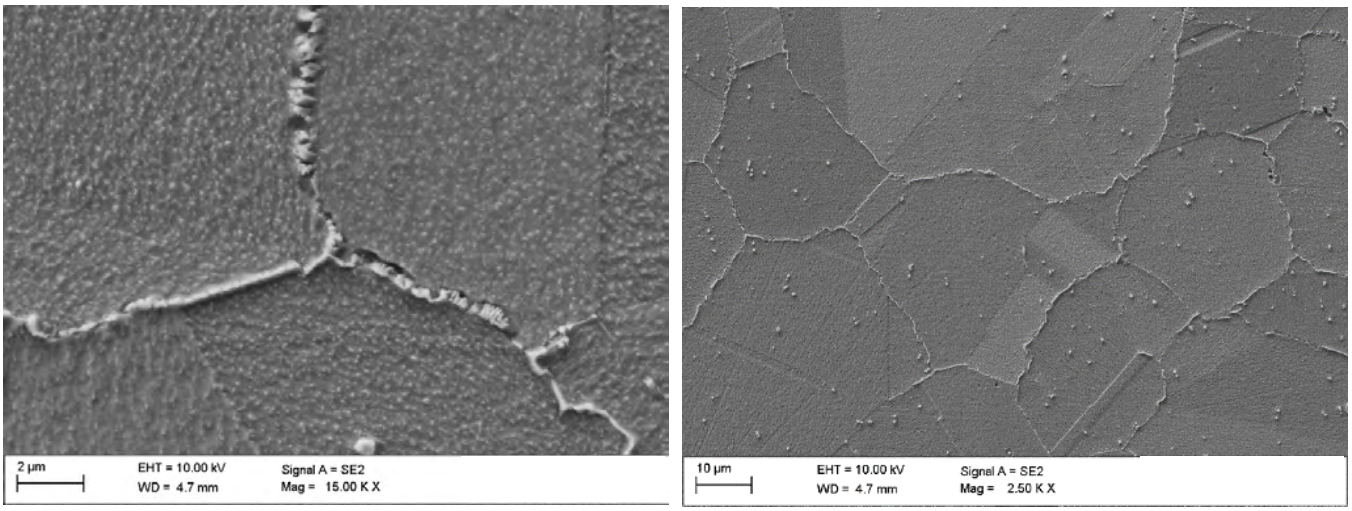

Figure 14: SEM images (SE mode) using Hydrochloric-Nitric-Acid (6:1) etching after an aging of 5000 h at 600°C.

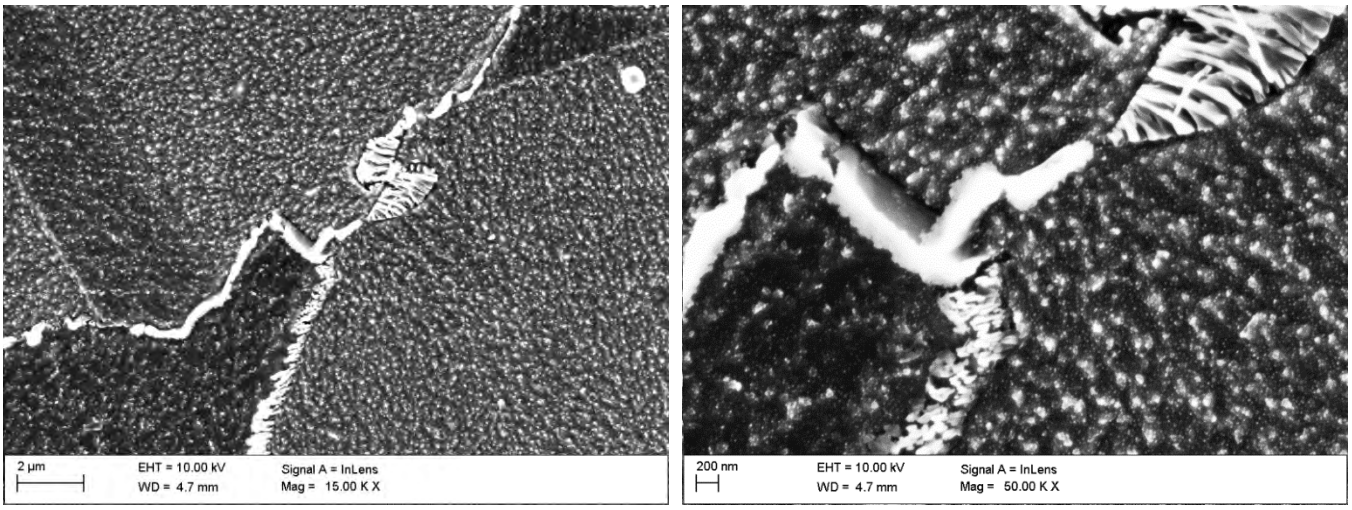

Figure 15: SEM images (InLens mode) using Hydrochloric-Nitric-Acid (6:1) etching after an aging of 5000 h at 600°C.

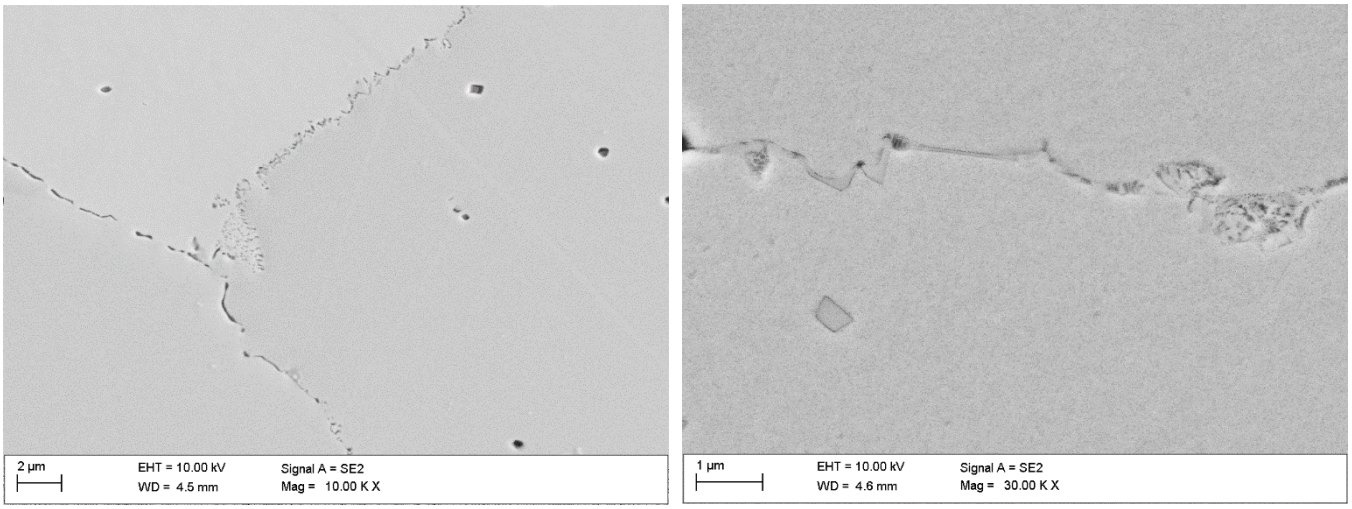

Figure 16: SEM images (SE mode) using Murakami's (left) and Canada's etching (right) after an aging of 5000 h at 600°C.

Figure 15 shows fine γ'-precipitations in the grains and carbide and γ'-precipitations on the grain boundaries. Figure 16 indicates fine γ'-precipitations in the grains. The γ'-phase can be etched out without "deep holes" in the matrix.

Aging at 700°C for 5000 h

After an exposure at 700°C for 5000 h a slight coarsening of carbide precipitations on the grain boundaries can be seen (Figure 17 and 20). The "zigzag" shape of grain boundaries is less present at this temperature (Figure 19). Also γ'-precipitations can be observed in the grains and on the grain boundaries (Figure 18), as illustrated in images with Canadas etching in Figure 20. The size of the γ'-precipitations is in the range of about 30 to 100 nm (see Figure 18 and 19). The γ'-phase in the grains is homogeneously distributed.

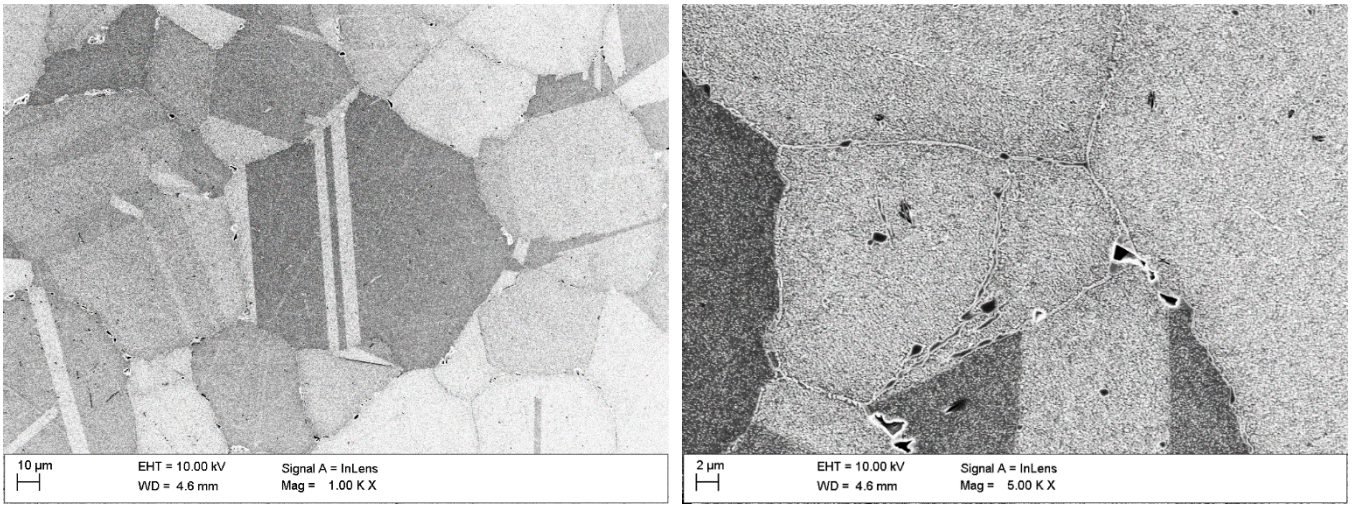

Figure 17: SEM images (InLens mode) using Hydrochloric-Nitric-Acid (6:1) etching after an aging of 5000 h at 700°C.

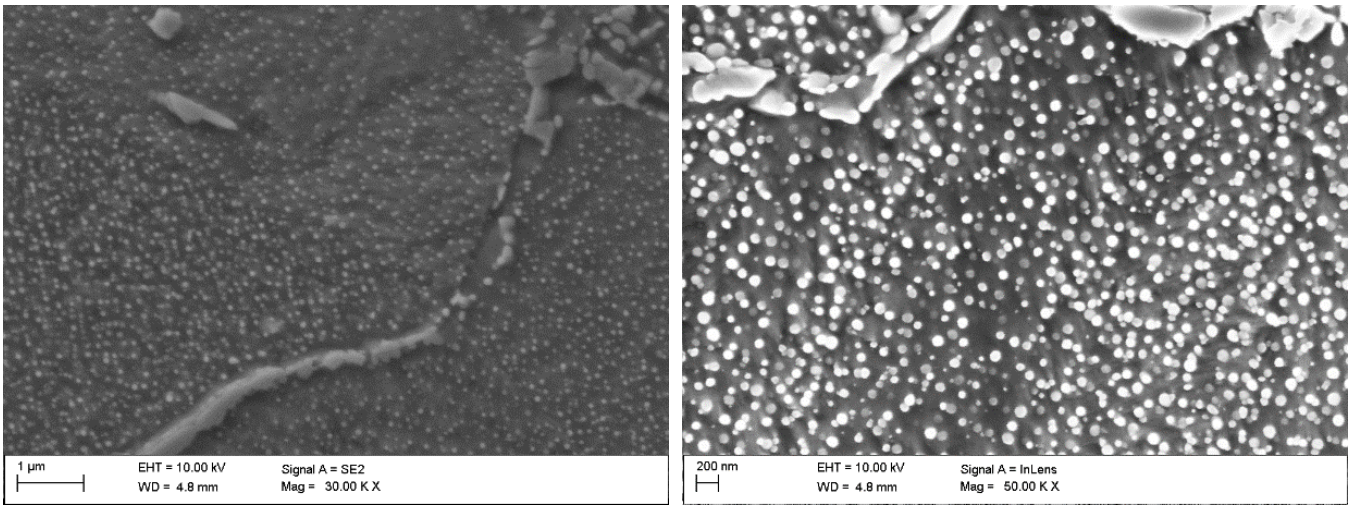

Figure 18: SEM images (SE mode) using Hydrochloric-Nitric-Acid (6:1) etching after an aging of 5000 h at 700°C.

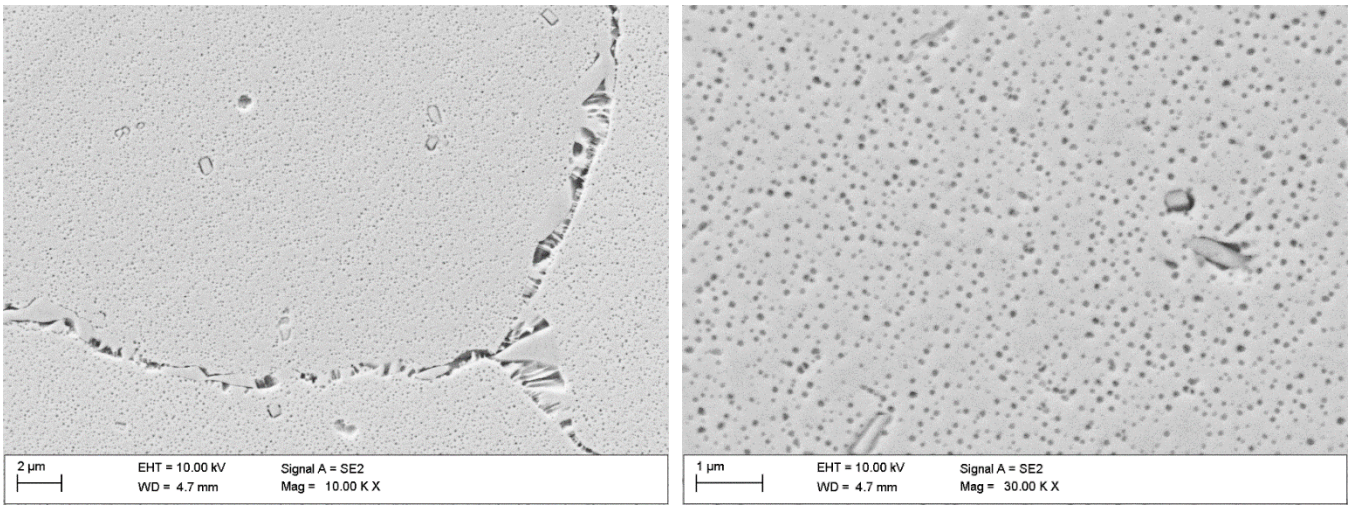

Figure 19: SEM images (SE mode) using Canada's etching after an aging of 5000 h at 700°C.

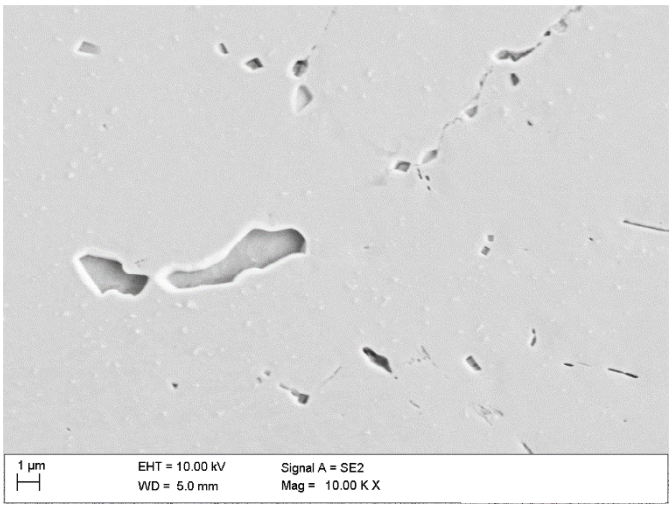

Figure 20: SEM images (SE mode) using Murakami's etching after an aging of 5000 h at 700°C.

Aging at 800°C for 2000 h

After an exposure at 800°C for 2000 h a stronger coarsening of carbide precipitations on the grain boundaries as well as γ'-precipitations in the grains can be observed (see Figure 21 to 23). In Figure 22 this coarsening of the γ' particles can be seen by using the Canadas etching. The regions near the grain boundaries seem to contain less γ'-precipitations in comparison to the middle of the grains. This and the coarsening of γ'-precipitations leads to a decreasing strengthening effect by the γ'-phase, which is illustrated in Figure 7, and hence to a reduction of the yield strength. According to the thermodynamical calculations in Figure 5 γ'-phase (solvus temperature about 770°C) should not be observed at 800°C, but these calculations have a certain inaccuracy, depending on the availability of experimental data in the alloying range. Such inaccuracies could be expected for the calculation of a new alloy like Alloy 699 XA. Nevertheless, the γ'-phase distribution changes according to a temperature slightly below the solvus temperature. In this temperature region, a small amount of coarser particles is expected. This result also fits to the results of the tensile tests in Figure 7, where during aging at 800°C the yield strength first increases and then decreases with increasing aging time.

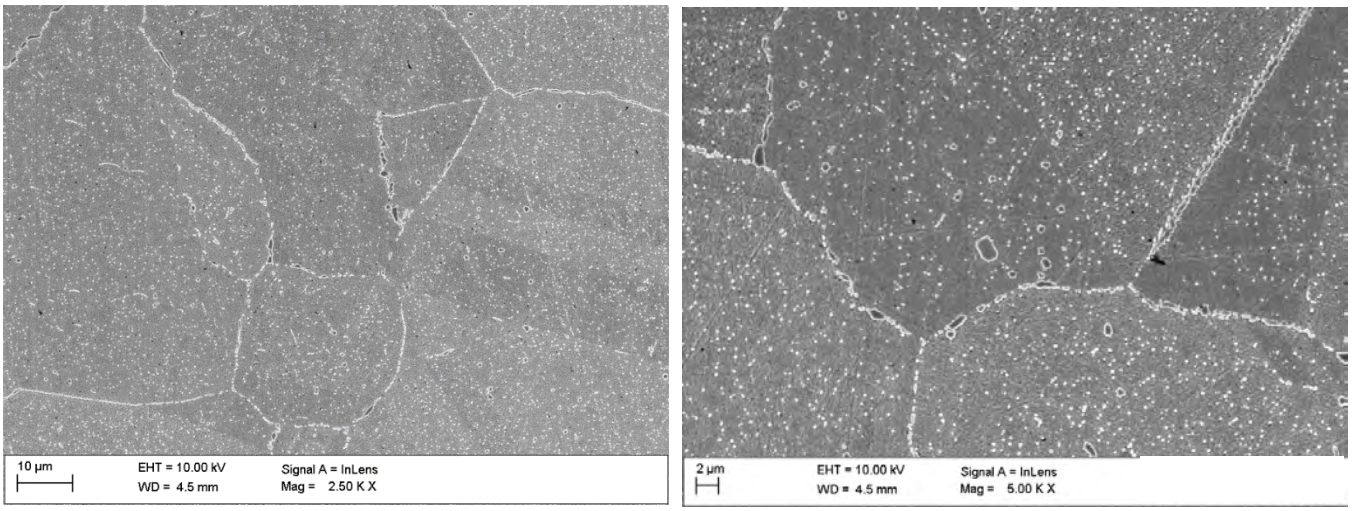

Figure 21: SEM images (InLens mode) using Hydrochloric-Nitric-Acid (6:1) etching after an aging of 2000 h at 800°C.

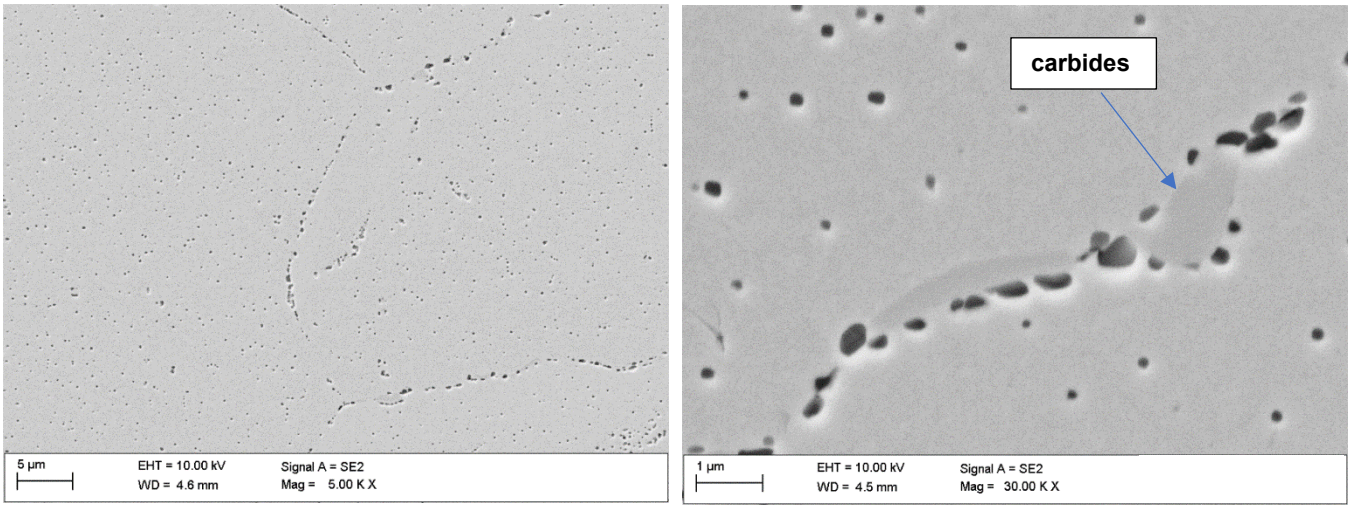

Figure 22: SEM images (SE mode) using Canada's etching after an aging of 2000 h at 800°C.

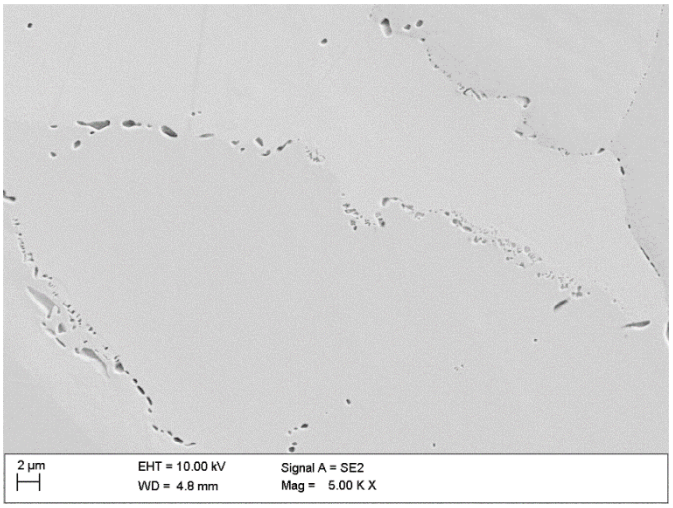

Figure 23: SEM images (SE mode) using Murakami's etching after an aging of 2000 h at 800°C.

Aging at 900°C for 2000 h

A further increase of the aging temperature to 900°C causes a dissolution of γ'-precipitations due to exceeding the solvus temperature. No γ'-phase can be seen in Figure 24 and 25 (left). Carbide precipitations on the grain boundaries become more globular (Figure 24 and 25).

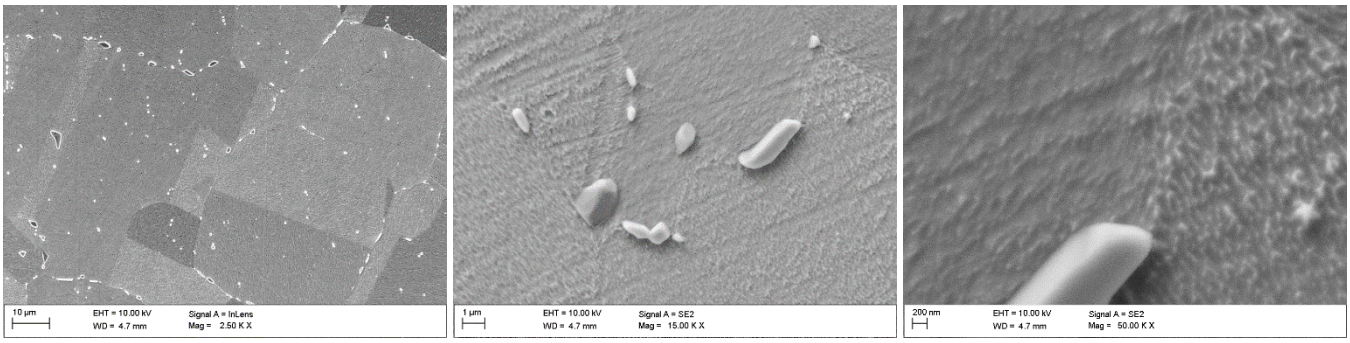

Figure 24: SEM images (InLens mode) using Hydrochloric-Nitric-Acid (6:1) etching after an aging of 2000 h at 900°C.

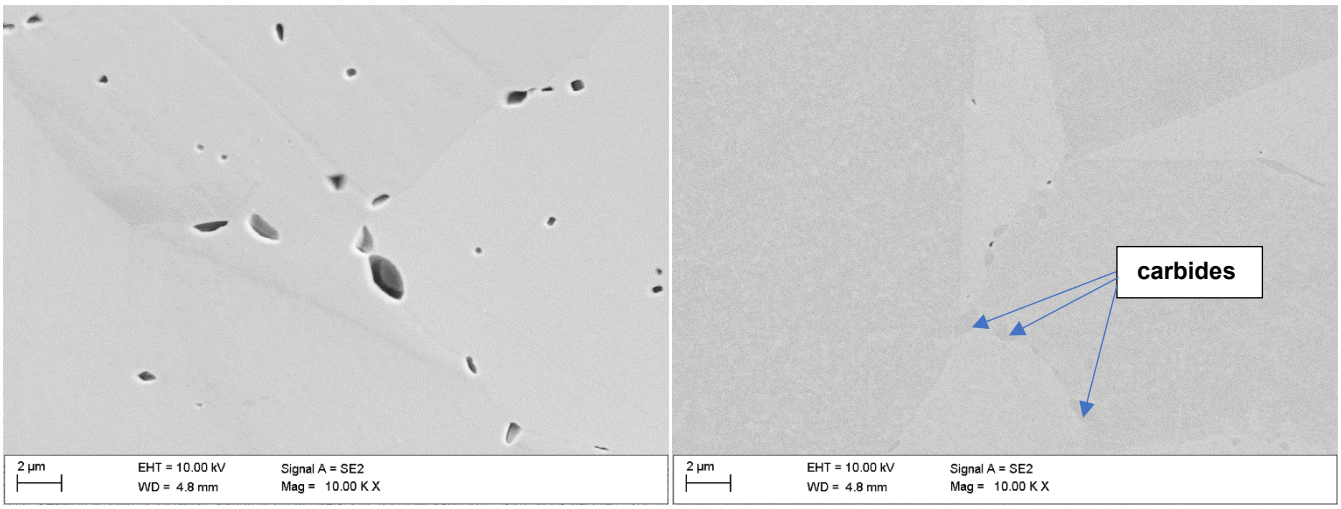

Figure 25: SEM images (SE mode) using Murakami's (left) and Canada's (right) etching after an aging of 2000 h at 900°C.

CONCLUSIONS

Microstructural investigations on Alloy 699 XA after long-term exposure at temperatures between 500 and 900°C for a duration up to 5000 h were presented in this study. The experimental results analyzed by SEM show that the solvus temperature of the γ'-phase is slightly above 800°C. This value is higher than the 770°C predicted by thermodynamic calculations with JMatPro simulation software. Such a deviation could be expected from thermodynamic calculation of a new alloy like 699 XA. The experimental results on aged samples analyzed by SEM are in coincidence with the results from mechanical tests. No detrimental phases or unfavorable phase morphologies have been identified. On grain boundaries carbides have been detected over the temperature range investigated. In the temperature range between 550 and 800°C γ'-precipitations on the grain boundaries were observed. Partly growing of γ'-phase precipitations through movement of grain boundaries ("zigzag" γ') was observed on the grain boundaries between 500 and 700°C. However, no continuous occupancy of one of the phases on the grain boundaries were detected, which could have a negative impact on the creep strength.

ACKNOWLEDGEMENTS

The authors would like to thank the colleagues of the mechanical laboratory at VDM Metals in Altena for the long time annealing treatments and the mechanical tests as well as Joachim Rösler and the members of the Institute of Materials Science (tu-braunschweig.de) for their support.

REFERENCES

1. F.A. Prange, “Corrosion in a Hydrocarbon Conversion System,” CORROSION/15, 12 (1959): pp 619 – 621
2. H. Hattendorf, A. López, J. Kloewer, “Alloy 699 XA – A New Alloy for Application under Metal Dusting Conditions,” CORROSION/2018, paper no. C2018-11200 (Phoenix AZ: Nace, 2018)
3. Wei-Ting Chen, Bingtao Li, Brian Gleeson, M. Galetz, Heike Hattendorf, “Characterization of Metal Dusting Corrosion of Ni-Based Alloy Ni29Cr2Al and its Weldment under Pressure Condition,“ CORROSION 2019 Symposium, March 24-28, 2019, Paper No.,: C2019-13258 Nashville, Tennessee, USA
4. JMatPro the Materials Properties Simulation Package Version 13, Sente Software Ltd. Surrey Technology Centre, 40 Occam Road, Guildford, Surray, GU2 7YG United Kingdom
5. DIN EN ISO 6892-1, „Metallische Werkstoffe- Zugversuch – Teil 1: Prüfverfahren bei Raumtemperatur (ISO 6892-1:2009, 2016 respectively)“, Deutsche Fassung EN ISO 6892-1:2009, 2016 respectively, (Berlin, Beuth Verlag GmbH, 2009, 2016 respectively)
6. Petzow, Günther, Metallographisches Ätzen, Gebrueder Borntraeger, Berlin, Stuttgart, 1976
7. Schmidt, P.F.: Praxis der Rasterelektronenmikroskopie und Mikrobereichsanalyse. Expert Verlag, Renningen, 1994.
8. Tatiana Hentrich, Heike Hattendorf, Alejandra Lopez, VDM® Alloy 699 XA, “A newly developed Alloy for Application under Metal Dusting Conditions”, *32. Nitrogen + Syngas 2019, Conference*, Berlin, 4 – 7.03.2019.
9. Bürgel, R. Handbuch Hochtemperatur-Werkstoffmechanik, Vieweg Verlag, Wiesbaden, 2006, p 136 – 150.
10. Donachie, Matthew J., Donachie, Stephen J., Superalloys - A Technical Guide, ASM International, USA, 2002, p 35 - 37